SUPPLEMENTARY INFORMATION

Supplementary information to the article "Cross-sectional brain age assessments predict future brain change", Korbmacher et al., 2024

Contents

2

SUPPLEMENTARY TABLES

Supplementary Table 1. Model performance for corrected and uncorrected predictions

LM Predictions	R^2	MAE	RMSE	Correlation	lower 95% CI	upper 95% CI	Correction
dMRI training	0.761	2.995	3.765	0.872	0.870	0.875	No
dMRI test visit 1	0.709	3.107	3.924	0.842	0.830	0.853	No
dMRI test visit 2	0.722	2.976	3.754	0.850	0.838	0.860	No
T1w MRI training	0.510	4.338	5.393	0.714	0.709	0.719	No
T1w MRI test visit 1	0.472	4.300	5.356	0.687	0.666	0.707	No
T1w MRI test visit 2	0.494	4.032	5.073	0.703	0.683	0.722	No
multimodal MRI training	0.779	2.885	3.619	0.883	0.881	0.885	No
multimodal MRI test visit 1	0.729	3.012	3.773	0.854	0.843	0.864	No
multimodal MRI test visit 2	0.739	2.893	3.644	0.860	0.849	0.870	No
dMRI training	0.993	1.329	1.605	0.996	0.996	0.996	Yes
dMRI test visit 1	0.991	1.301	1.572	0.996	0.995	0.996	Yes
dMRI test visit 2	0.991	1.237	1.490	0.996	0.995	0.996	Yes
T1w MRI training	0.963	2.165	2.696	0.981	0.981	0.982	Yes
T1w MRI test visit 1	0.963	2.039	2.517	0.981	0.980	0.983	Yes
T1w MRI test visit 2	0.958	2.104	2.622	0.979	0.977	0.981	Yes
multimodal MRI training	0.994	1.243	1.501	0.997	0.997	0.997	Yes
multimodal MRI test visit 1	0.992	1.215	1.469	0.996	0.996	0.996	Yes
multimodal MRI test visit 2	0.993	1.171	1.413	0.996	0.996	0.997	Yes

R^2 = variance explained, MAE = Mean Absolute Error, RMSE = Root Mean Squared Error, 95% CI = 95% Confidence Interval.

Supplementary Table 2. Brain age gap correlations (crude) between time points

Modality	Variable	Correlation	Lower 95% CI	Upper 95% CI
dMRI	Predicted Age	0.926	0.920	0.932
dMRI	Corrected Predicted Age	0.993	0.992	0.993
dMRI	BAG	0.814	0.800	0.827
dMRI	Corrected BAG	0.926	0.920	0.932
T1w MRI	Predicted Age	0.912	0.905	0.918
T1w MRI	Corrected Predicted Age	0.988	0.987	0.989
T1w MRI	BAG	0.909	0.902	0.916
T1w MRI	Corrected BAG	0.912	0.905	0.918
multimodal MRI	Predicted Age	0.934	0.929	0.939
multimodal MRI	Corrected Predicted Age	0.998	0.998	0.998
multimodal MRI	BAG	0.807	0.793	0.820
multimodal MRI	Corrected BAG	0.934	0.929	0.939

95% CI = 95% Confidence Interval.

Supplementary Table 3. Time point differences in brain age gaps

	Beta	SE	p	R^2m	R^2c	Mean TP1	Mean TP2
dMRI Uncorrected	0.324	0.051	2.20×10^{-10}	0.250	0.815	0.419	0.093
dMRI Corrected	0.077	0.012	2.20×10^{-10}	0.724	0.932	-0.513	-0.007
T1w Uncorrected	0.461	0.049	1.46×10^{-20}	0.492	0.912	1.064	0.291
T1w Corrected	0.226	0.024	1.46×10^{-20}	0.497	0.913	-0.737	0.082
multimodal Uncorrected	2.318	0.046	$<2.47\times10^{-324}$	0.283	0.824	-2.119	0.199
multimodal Corrected	0.511	0.010	$<2.47\times10^{-324}$	0.740	0.936	-0.495	0.017

The raw (unstandardized beta values) time point differences were corrected for age, sex, the interaction between age and sex, as well as the scanner site.
R^2m refers to marginal variance explained and R^2c refers to conditional variance explained.

Supplementary Table 4. Associations between cross-section and longitudinal measures (Principal Components and BAGs)

	Beta	Std. Beta	SE	t	p
dMRI corrected BAG	0.007	0.044	0.003	2.219	0.027
T1w corrected BAG	0.028	0.148	0.005	5.487	4.49×10^{-8}
Multimodal corrected BAG	0.001	0.009	0.006	0.235	0.814
dMRI uncorrected BAG	-0.016	-0.057	0.005	-2.855	0.004
T1w uncorrected BAG	0.028	0.147	0.005	5.475	4.81×10^{-8}
Multimodal uncorrected BAG	0.001	0.005	0.006	0.235	0.814
dMRI PC	-0.063	-0.081	0.015	-4.075	4.75×10^{-5}
T1w PC	-0.001	-0.002	0.018	-0.077	0.938
Multimodal PC	-0.054	-0.069	0.017	-3.205	0.001

Std. Beta indicates the standardized β coefficients, SE the Standard Error. All brain age gap (BAG) associations are between the centercept of the BAG ($\bar{BAG}$), i.e. the cross-sectional BAG, and the annual rate of change of BAG a(ΔBAG) i.e., the longitudinal BAG. Similarly, all principal component (PC) associations were between the centercept of the PC ($\bar{PC}$), i.e. the cross-sectional PC, and the annual rate of change PC (ΔPC) i.e., the longitudinal PC. The associations were controlled for the inter-scan interval, age, sex, the age-sex interaction, and the scanner/acquisition site. For completion, we also include a table for the effects when modelling the interaction effect with a cubic spline with k = 4 knots, using generalised additive models. F and p values in the last two columns on the right indicate the test statistics for the non-linear interaction effects. The left side of the table can be read as the table above.

	Effect of the centercept				Interaction Term	
	Std.Beta	SE	t	p	F	p
dMRI corrected BAG	0.044	0.020	2.224	0.026	1.405	0.318
T1w corrected BAG	0.145	0.027	5.354	9.39×10^{-8}	1.953	0.126
multimodal corrected BAG	0.005	0.039	0.136	0.892	1.798	0.090
dMRI uncorrected BAG	-0.059	0.020	-2.941	0.003	2.950	0.028
T1w uncorrected BAG	0.145	0.027	5.382	8.04×10^{-8}	2.363	0.089
multimodal uncorrected BAG	0.009	0.022	0.414	0.679	3.592	0.010
dMRI PC	-0.081	0.020	-4.097	4.33×10^{-5}	2.295	0.092
T1w PC	0.003	0.023	0.131	0.896	2.651	0.050
multimodal PC	-0.068	0.022	-3.171	0.002	5.436	0.020

Supplementary Table 5. Associations between cross-section and longitudinal measures (Principal Components and BAGs) accounting for the interaction of the inter-scan interval and $\bar{BAG}$

	Sex-ISI Interaction				Centercept			
	Std. Beta	SE	t	p	Std. Beta	SE	t	p
dMRI corrected BAG	-0.005	0.025	-0.186	0.852	0.056	0.066	0.852	0.394
T1w corrected BAG	-0.001	0.025	-0.055	0.956	0.151	0.067	2.266	0.024
multimodal corrected BAG	0.022	0.028	0.785	0.432	-0.045	0.079	-0.565	0.572
dMRI uncorrected BAG	-0.032	0.031	-1.040	0.298	0.021	0.078	0.271	0.786
T1w uncorrected BAG	0.004	0.025	0.163	0.871	0.137	0.067	2.056	0.040
multimodal uncorrected BAG	-0.027	0.026	-1.041	0.298	0.072	0.067	1.060	0.289
dMRI PC	-0.016	0.025	-0.632	0.527	-0.042	0.065	-0.634	0.526
T1w PC	0.006	0.026	0.227	0.821	-0.016	0.067	-0.240	0.811
multimodal PC	0.062	0.027	2.331	0.020	-0.221	0.069	-3.223	0.001

Table 1 Statistical analysis of BAG and PC models in corrected and uncorrected forms

ISI indicates the Inter-Scan Interval, Std. Beta indicates the standardized β coefficients, SE the Standard Error. All brain age gap (BAG) associations are between the centercept of the BAG ($\bar{BAG}$), i.e. the cross-sectional BAG, and the annual rate of change of BAG a(ΔBAG) i.e., the longitudinal BAG. Similarly, all principal component (PC) associations were between the centercept of the PC ($\bar{PC}$), i.e. the cross-sectional PC, and the annual rate of change PC (ΔPC) i.e., the longitudinal PC. The associations were controlled for the inter-scan interval (and the interaction between the inter-scan interval and the respective cross-sectional measure), age, sex, the age-sex interaction, and the scanner/acquisition site.

Supplementary Table 6. Associations between Brain Age Gaps (longitudinal and cross-sectional) and Principal Components (longitudinal and cross-sectional)

Variable Pair	Std. Beta	SE	t	p
corrected $B\bar{A}G$_dMRI & ΔPC_dMRI	-0.083	0.020	-4.190	2.88×10^{-5}
corrected $B\bar{A}G$_dMRI & $\bar{PC}$_dMRI	0.483	0.017	27.673	2.33×10^{-147}
corrected $B\bar{A}G$_T1w & ΔPC_T1w	0.054	0.015	3.549	3.94×10^{-4}
corrected $B\bar{A}G$_T1w & $\bar{PC}$_T1w	0.319	0.016	19.727	1.19×10^{-80}
corrected $B\bar{A}G$_multi & ΔPC_multi	0.002	0.010	0.170	0.865
corrected $B\bar{A}G$_multi & $\bar{PC}$_multi	0.154	0.010	14.740	3.15×10^{-47}
uncorrected $B\bar{A}G$_dMRI & ΔPC_dMRI	0.046	0.020	2.322	0.020
uncorrected $B\bar{A}G$_dMRI & $\bar{PC}$_dMRI	0.004	0.020	0.187	0.852
uncorrected $B\bar{A}G$_T1w & ΔPC_T1w	0.054	0.015	3.549	3.94×10^{-4}
uncorrected $B\bar{A}G$_T1w & $\bar{PC}$_T1w	0.317	0.016	19.727	1.19×10^{-80}
uncorrected $B\bar{A}G$_multi & ΔPC_multi	0.003	0.018	0.170	0.865
uncorrected $B\bar{A}G$_multi & $\bar{PC}$_multi	0.273	0.019	14.740	3.15×10^{-47}
corrected ΔBAG_dMRI & ΔPC_dMRI	0.004	0.020	0.224	0.823
corrected ΔBAG_dMRI & $\bar{PC}$_dMRI	0.011	0.020	0.571	0.568
corrected ΔBAG_T1w & ΔPC_T1w	0.492	0.018	26.873	4.93×10^{-140}
corrected ΔBAG_T1w & $\bar{PC}$_T1w	0.040	0.024	1.719	0.086
corrected ΔBAG_multi & ΔPC_multi	0.010	0.020	0.518	0.605
corrected ΔBAG_multi & $\bar{PC}$_multi	-0.024	0.021	-1.109	0.267
uncorrected ΔBAG_dMRI & ΔPC_dMRI	0.004	0.020	0.224	0.823
uncorrected ΔBAG_dMRI & $\bar{PC}$_dMRI	0.011	0.020	0.571	0.568
uncorrected ΔBAG_T1w & ΔPC_T1w	0.434	0.019	23.108	2.75×10^{-107}
uncorrected ΔBAG_T1w & $\bar{PC}$_T1w	0.035	0.023	1.503	0.133
uncorrected ΔBAG_multi & ΔPC_multi	0.010	0.020	0.518	0.605
uncorrected ΔBAG_multi & $\bar{PC}$_multi	-0.024	0.021	-1.109	0.267

The associations were controlled for the inter-scan interval, age, sex, the age-sex interaction, and the scanner/acquisition site.

Supplementary Table 7. Model performance comparison

Model	r2	MAE	RMSE	cor	CI95l	CI95u
LM T1 training	0.510	4.338	5.393	0.714	0.709	0.719
LM T1 TP1	0.472	4.530	5.356	0.687	0.669	0.707
LM T1 TP2	0.482	4.574	5.345	0.687	0.669	0.706
LM dMRI training	0.761	2.995	3.915	0.872	0.870	0.875
LM dMRI TP1	0.709	3.197	4.027	0.829	0.812	0.847
LM dMRI TP2	0.722	2.976	3.879	0.844	0.823	0.863
LM multi training	0.779	2.855	3.564	0.883	0.880	0.884
LM multi TP1	0.773	2.985	3.554	0.883	0.869	0.893
LM multi TP2	0.739	2.893	3.581	0.864	0.847	0.880
XGB T1 training	0.694	3.121	4.003	0.764	0.761	0.768
XGB T1 TP1	0.583	3.389	4.367	0.640	0.615	0.664
XGB T1 TP2	0.575	3.634	4.516	0.620	0.593	0.644
XGB dMRI training	0.704	2.975	3.837	0.776	0.771	0.781
XGB dMRI TP1	0.605	3.298	4.246	0.676	0.652	0.699
XGB dMRI TP2	0.582	3.449	4.369	0.670	0.648	0.691
XGB multi training	0.722	2.895	3.646	0.797	0.794	0.801
XGB multi TP1	0.597	3.172	4.192	0.773	0.746	0.797
XGB multi TP2	0.575	3.438	4.360	0.783	0.767	0.794
Lasso T1 training	0.470	4.156	5.345	0.687	0.683	0.690
Lasso T1 TP1	0.536	4.374	5.157	0.715	0.698	0.732
Lasso T1 TP2	0.616	3.745	4.878	0.746	0.730	0.760
Lasso dMRI training	0.695	2.943	3.726	0.780	0.776	0.784
Lasso dMRI TP1	0.659	3.279	4.133	0.752	0.735	0.770
Lasso dMRI TP2	0.693	2.820	3.723	0.780	0.767	0.791
Lasso multi training	0.790	2.840	3.465	0.895	0.892	0.899
Lasso multi TP1	0.676	3.198	3.992	0.794	0.782	0.801
Lasso multi TP2	0.631	3.746	4.686	0.794	0.791	0.798

Supplementary Table 8. White matter features by diffusion approaches

Diffusion Approach	Metrics
Bayesian Rotationally Invariant Approach (BRIA)[1]	intra-axonal axial diffusivity (DAX intra)
	extra-axonal radial diffusivity (DRAD extra)*
	microscopic fractional anisotropy (micro FA)
	extra-axonal axial diffusivity (DAX extra)
	intra-axonal water fraction (V intra)
	extra-axonal water fraction (V extra)
	cerebrospinal fluid fraction (vCSF)
	microscopical axial diffusivity (micro AX)
	microscopic radial diffusivity (micro RD)
	microscopical apparent diffusion coefficient (micro ADC)
Diffusion Kurtosis Imaging (DKI)[2, 3]	mean kurtosis (MK)
	radial kurtosis (RK)
	axial kurtosis (AK)
Diffusion Tensor Imaging (DTI)[4]	fractional anisotropy (FA)
	axial diffusivity (AD)
	mean diffusivity (MD)
	radial diffusivity (RD)
Spherical Mean Technique (SMT)[5]	fractional anisotropy (SMT FA)
	mean diffusivity (SMT md)
	transverse diffusion coefficient (SMT trans)
	longitudinal diffusion coefficient (SMT long)
Multi-compartment Spherical Mean Technique (SMTmc)[6]	extra-neurite microscopic
	mean diffusivity (SMTmc extra md)
	extra-neurite transverse microscopic diffusivity (SMTmc extra trans)
	mc SMTdiffusion coefficient (SMT mcd)
	intra-neurite volume fraction (SMTmc intra)
White Matter Tract Integrity (WMTI)[3]	axonal water fraction (AWF)
	radial extra-axonal diffusivity (radEAD)
	axial extra-axonal diffusivity (axEAD)*

*Note that Drad extra and axEAD were excluded from the analyses as a significant portion of the produced metrics did not pass our quality control procedure[7].

Supplementary Table 9. Exploration of time point isolated BAG

Variable	Value
predicted age difference	2.540
corrected predicted age difference	1.440
age difference	2.560
brain age gap time point 1	-0.099
brain age gap time point 2	-0.118
corrected brain age gap time point 1	-0.183
corrected brain age gap time point 2	-0.057
t-test pval	0.819
LMER pval	1.205×10^{-40}
LMER beta	1.260
Marginal means difference	2.5

We estimated brain age at each time point independently for T_1-weighted MRI data for the same individuals. The other modalities were not used due to the large number of features in contrast to the relatively low number of degrees of freedom.

The decrease in uncorrected BAG indicated in the table, indicates that participants' brains were on average younger at time point 2 compared to time point 1, which is in conflict with the findings presented in the main text as well as potential ageing processes which might be captured by the BAG. On the other hand, the corrected BAG could capture a BAG towards a more positive value (higher predicted compared to chronological age), which is in line with the findings presented in the main text and Suppl.Table 3. This was also reflected by the linear mixed effect model (LMER) which indicated an annual change in brain age of 1.26 years, suggesting an increasing BAG over time.

While the same direction of effects were capture by these time point isolated models, their magnitude might be overestimated. This might be due to the larger uncertainty during training and testing, as the sample sizes were smaller. This underscores the importance of using models which are trained on large-scale data. When attempting to predict in longitudinal data.

Supplementary Table 10. Exploration of time point isolated *uncorrected* age predictions across time point specific models

| Prediction	Predicted Age	Chronological Age	BAG
TP1 to TP1	62.002	62.223	-0.099
TP2 to TP2	64.543	64.668	-0.118
TP1 to TP2	62.858	62.223	0.757
TP2 to TP1	63.414	64.668	-1.247

The table shows the results of models trained on longitudinal data only using the data points of the same subjects to train models on each respective time point and then predicting within the same time point or towards the other time point. The results indicate a reduction in BAG, indicating a reversed brain ageing, likely due to modelling error. This contrasts the predictions presented in the main text and questions the utility of models predicting across time points.

Supplementary Table 11. Exploration of time point isolated *corrected* age predictions across time point specific models

Prediction	Corrected Predicted Age	Chronological Age	Corrected BAG
TP1 to TP1	61.918	62.223	-0.183
TP2 to TP2	64.604	64.668	-0.057
TP1 to TP2	66.213	62.223	1.552
TP2 to TP1	60.630	64.668	-1.471

The table shows the results of models trained on longitudinal data only using the data points of the same subjects to train models on each respective time point and then predicting within the same time point or towards the other time point. The results indicate a reduction in the corrected BAG when predicted by models trained on data from another time point, indicating reversed brain aging, likely due to modeling error. This contrasts both the predictions within a single time point and the predictions presented in the main text and questions the utility of models predicting across time points.

# Supplementary Table 12. Standardised BAG time point differences

	Beta	SE	p	R2m	R2c
dMRI Uncorrected	0.085	0.013	2.2×10^{-10}	0.250	0.815
dMRI Corrected	0.051	0.008	2.2×10^{-10}	0.724	0.932
T1w Uncorrected	0.089	0.010	1.46×10^{-20}	0.492	0.912
T1w Corrected	0.089	0.009	1.46×10^{-20}	0.497	0.913
multimodal Uncorrected	0.597	0.012	$<2.47 \times 10^{-324}$	0.283	0.824
multimodal Corrected	0.360	0.007	$<2.47 \times 10^{-324}$	0.740	0.936

SUPPLEMENTARY FIGURES

Supplementary Figure 1. Scree Plots for the Principal Components Analyses
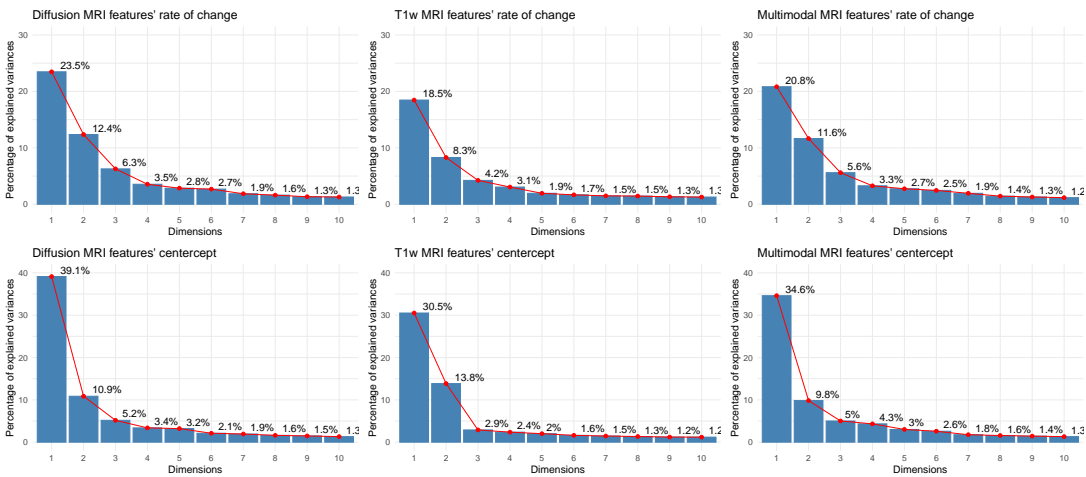
Supplementary Figure 2. Contour plots visualising the interaction effect of inter-scan interval and cross-sectional BAG on the annual rate of change of BAG
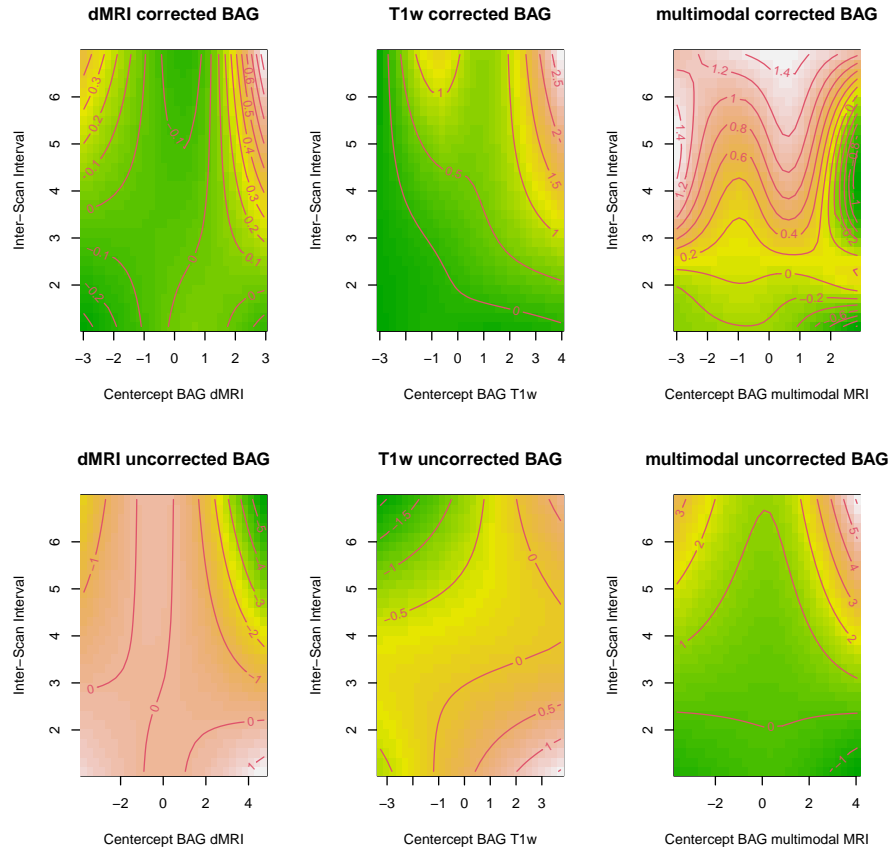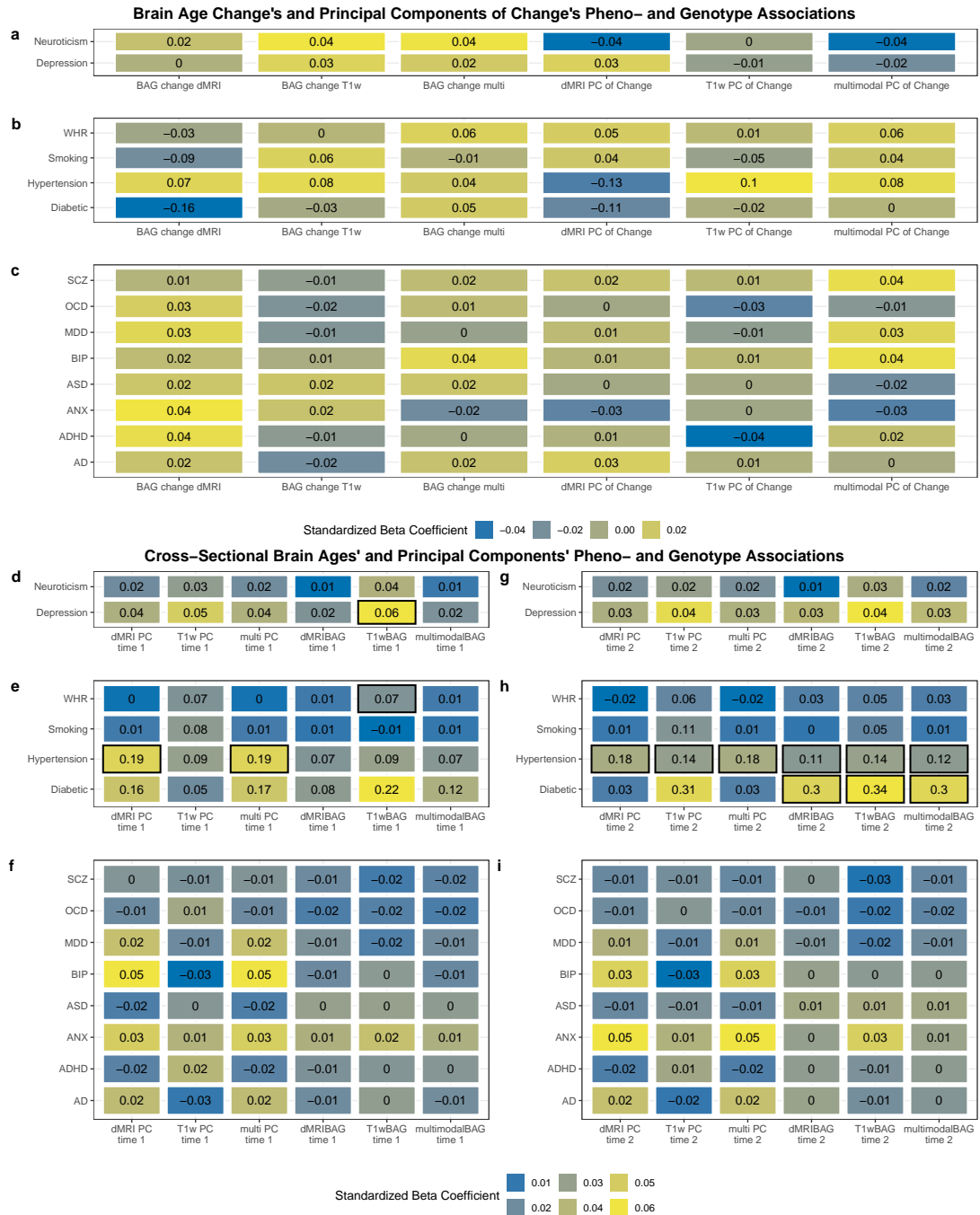
Supplementary Figure 3. Relative contribution of features to the first two principal components for each modality
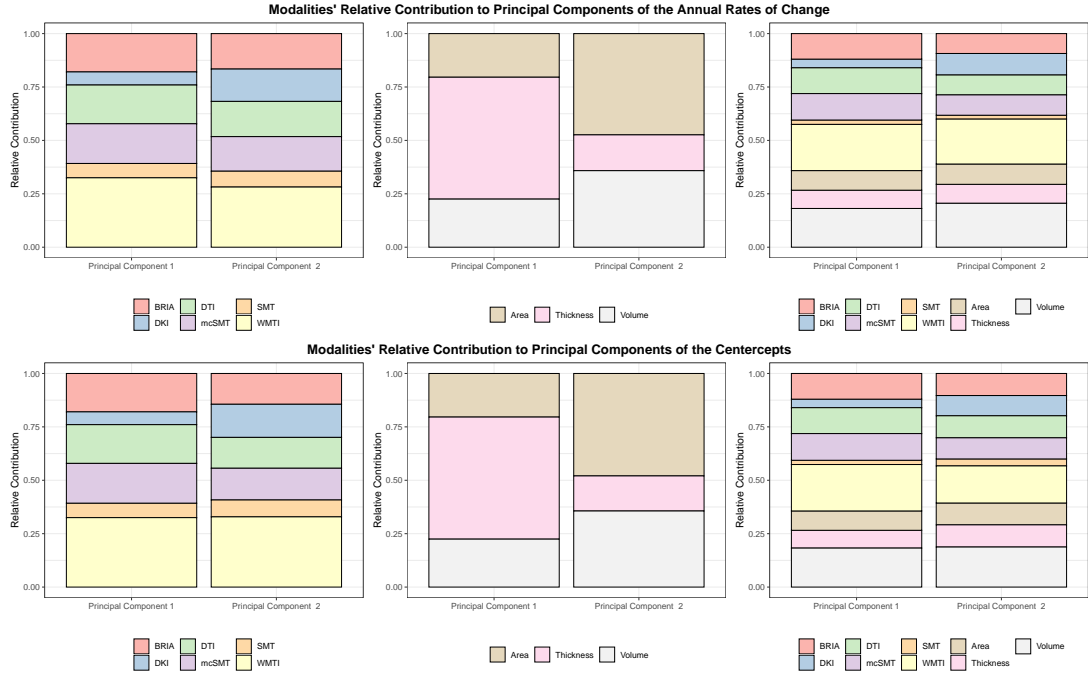
Panels from left to right: Diffusion MRI, T$_1$-weighted MRI, multimodal MRI. Diffusion features were derived using different approaches, including Diffusion Tensor Imaging (DTI) [4], Diffusion Kurtosis Imaging (DKI) [2], White Matter Tract Integrity (WMTI) [3], Spherical Mean Technique (SMT) [5], and multi-compartment Spherical Mean Technique (mcSMT)[6], and the Bayesian Rotational Invariant Approach (BRIA)[1].

Supplementary Figure 4. Associations between PCs, BAG, annual BAG and PC change, and pheno- and geno-types of health

Brain Age Change's and Principal Components of Change's Pheno- and Genotype Associations

Cross-Sectional Brain Ages' and Principal Components' Pheno- and Genotype Associations

a) Associations between the annual change in multimodal principal components (PCs) and brain age gaps (BAGs) with neuroticism and depression. b) Associations between the annual change in multimodal PCs and BAGs with cardiometabolic risk factors. WHR = waist to hip ratio, Smoking (yes/no), Hypertension (yes/no), Diabetes (yes/no). c) Associations between the annual change in multimodal PCs and BAGs with polygenic risk scores of psychiatric disorders and Alzheimer's disease. SCZ = schiziphrenia, OCD = obsessive compulsive disorder, MDD = major depressive disorder, BP = bipolar disorder, ASD = autism spectrum disorder, ANX = anxiety disorder, ADHD = attention deficit hyperactivity disorder, AD = Alzheimer's Disease. d-e) Associations as presented in a-c) but with cross-sectional measures of PCs and BAGs.

Note: Framed boxes indicate an FDR-corrected p < 0.05. Colours indicate the direction of the associations (blue = negative, yellow = positive). The effect sizes (standardised beta coefficients) are indicated in each box.

Supplementary Figure 5. Time point differences in features by T1-weighted metrics and diffusion approaches
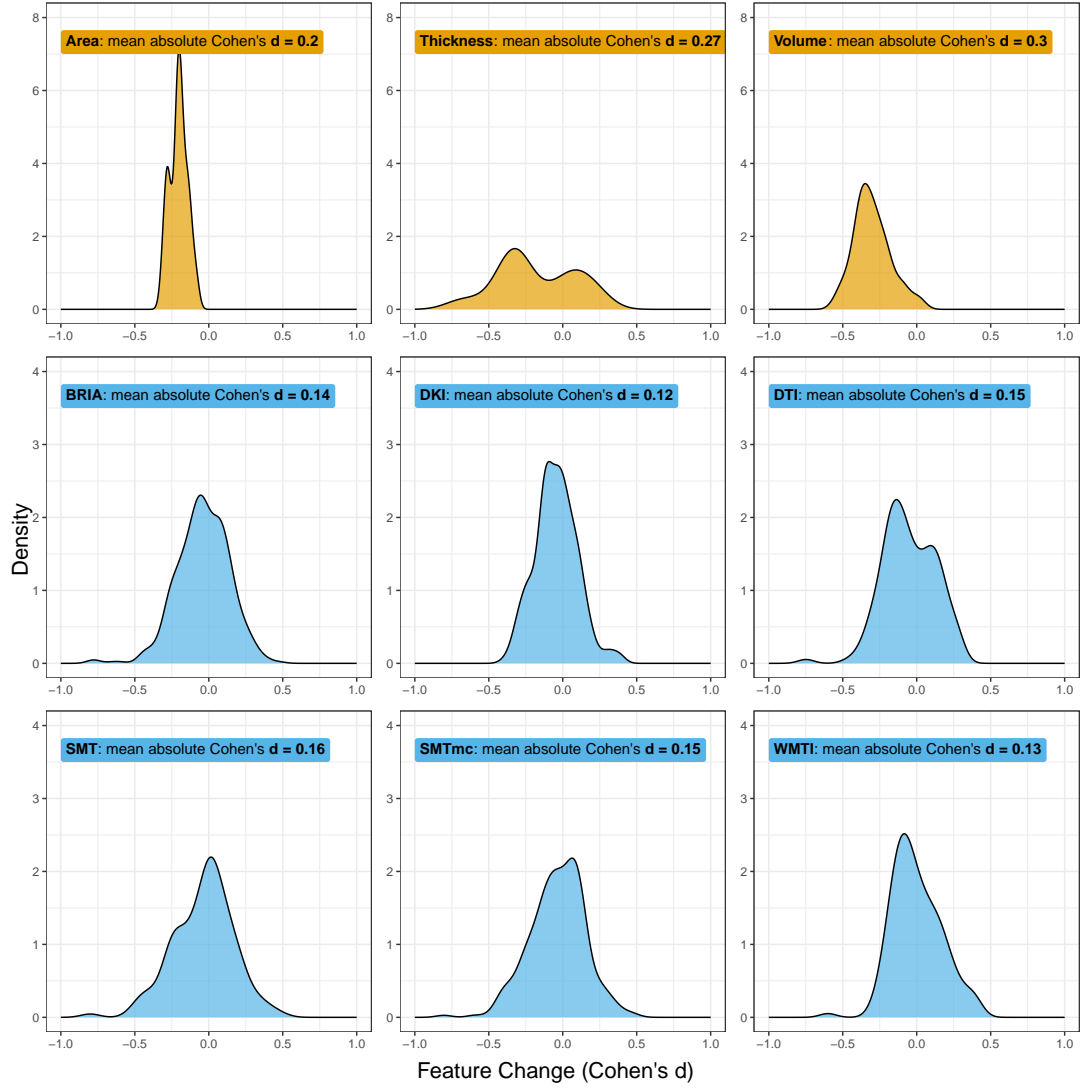
The top row shows the distribution of time point differences in $T_1 - weighted$ MRI derived metrics. The bottom two rows show the distribution of time point differences in all metrics entailed in each of the selected dMRI approaches.
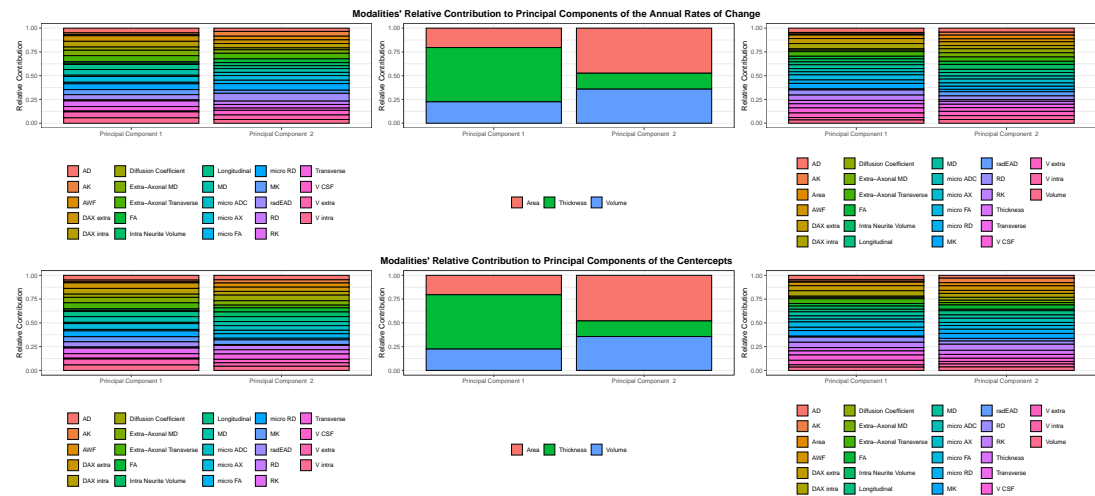
# Supplementary Figure 6. Time point differences in features by processing approach
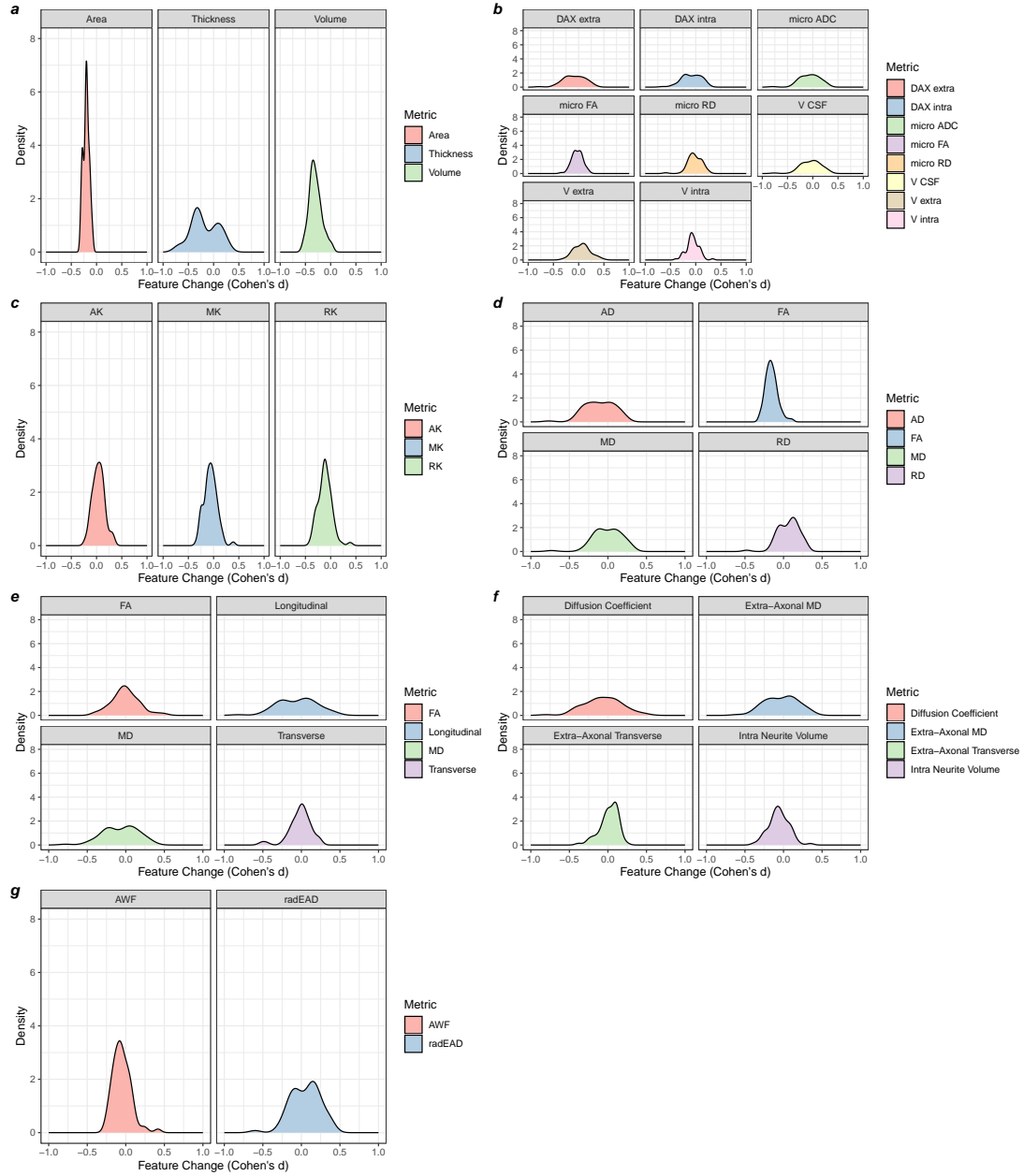
The figure presents the distribution of regional changes in different metrics. a) T_1w MRI derived metrics, b) metrics from the Bayesian Rotationally Invariant Approach,

c) metrics from Diffusion Kurtosis Imaging, d) metrics from Diffusion Tensor Imaging, e) metrics derived using the Spherical Mean Technique, f) metrics derived using the multi-compartment variant of Spherical Mean Technique, g) metrics from the White Matter Tract Integrity approach.

Supplementary Figure 7. Relative contributions of feature types to principal components by modality

Modalities' Relative Contribution to Principal Components of the Annual Rates of Change

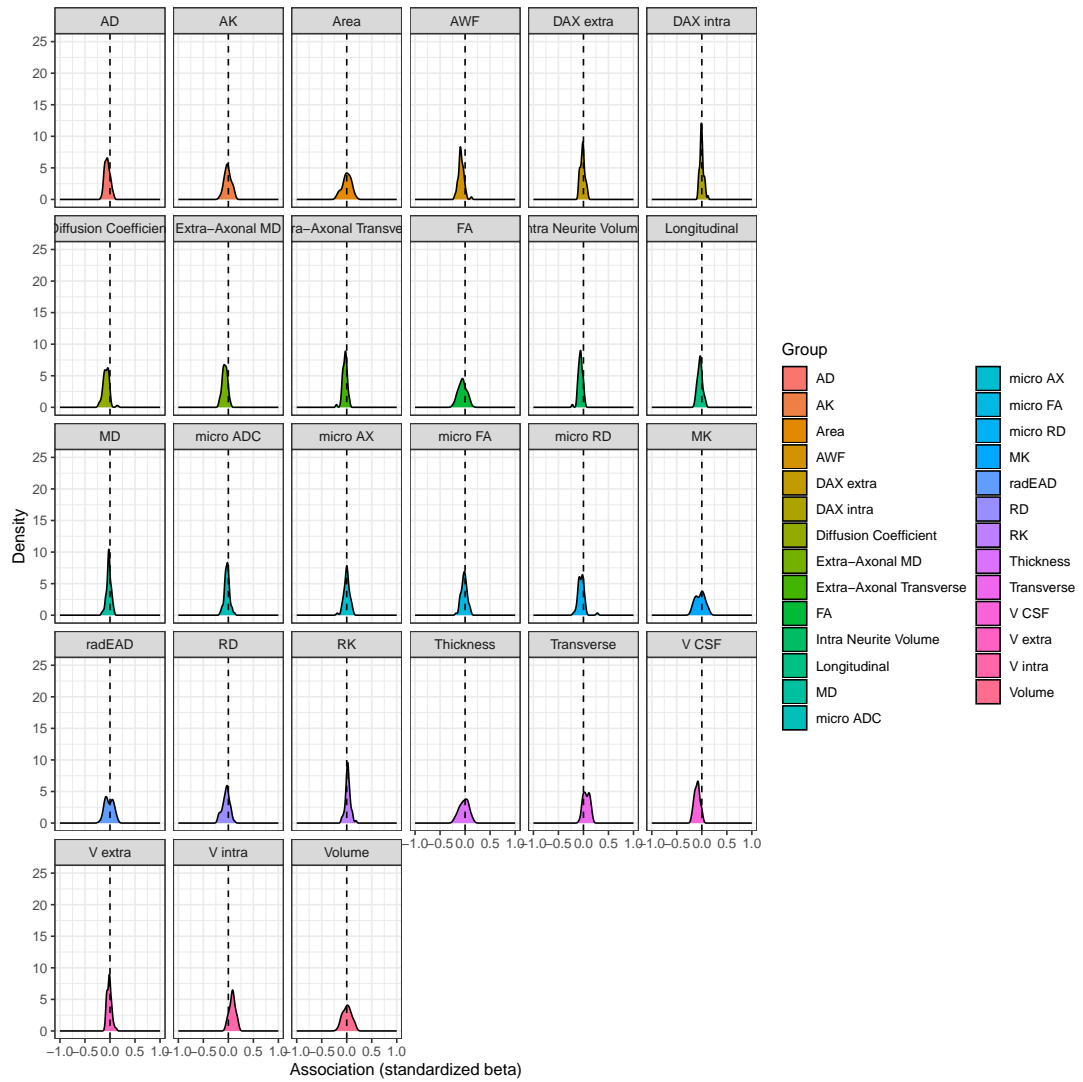Modalities' Relative Contribution to Principal Components of the Centercepts

Supplementary Figure 8. dMRI centercept BAG associations with the rate of change in dMRI features
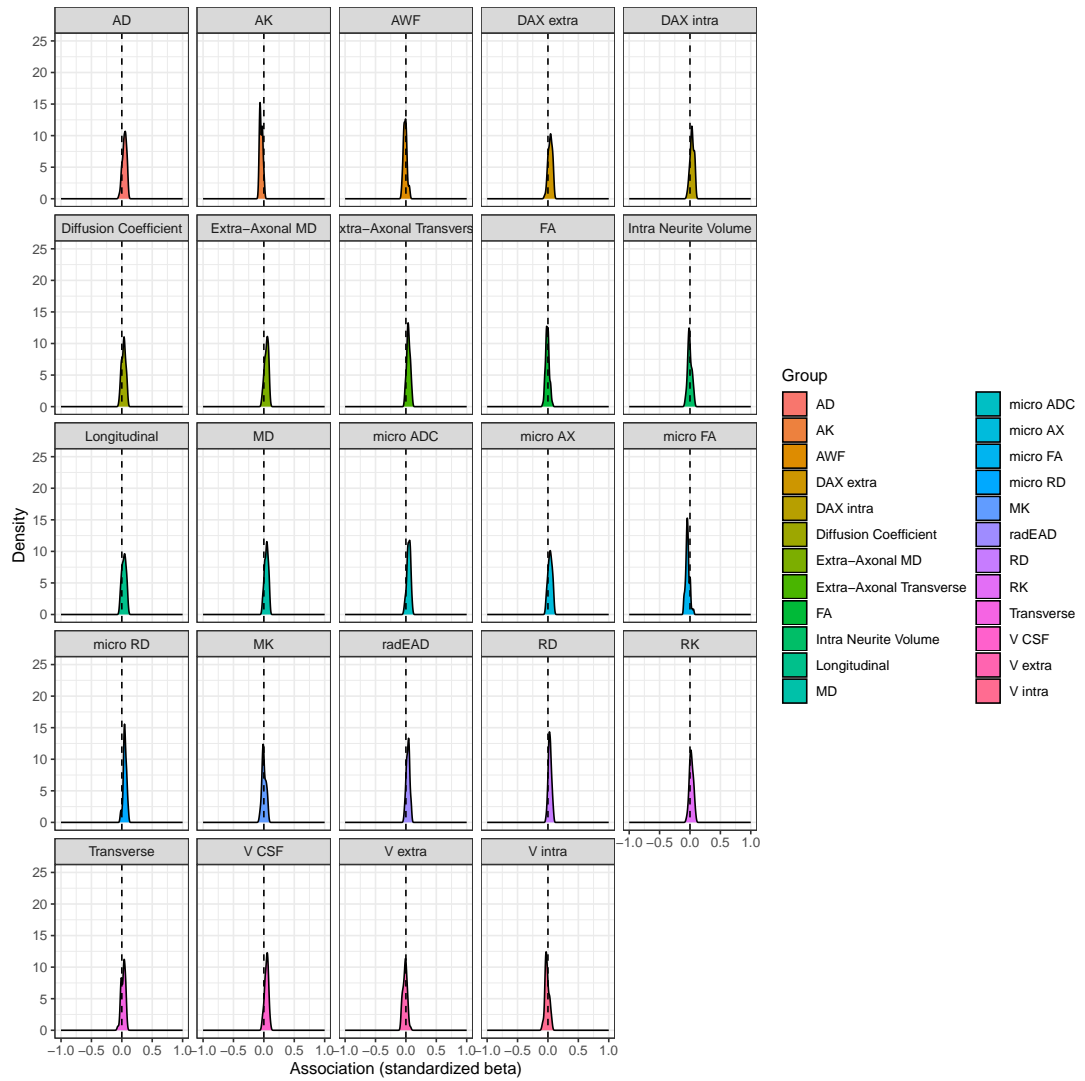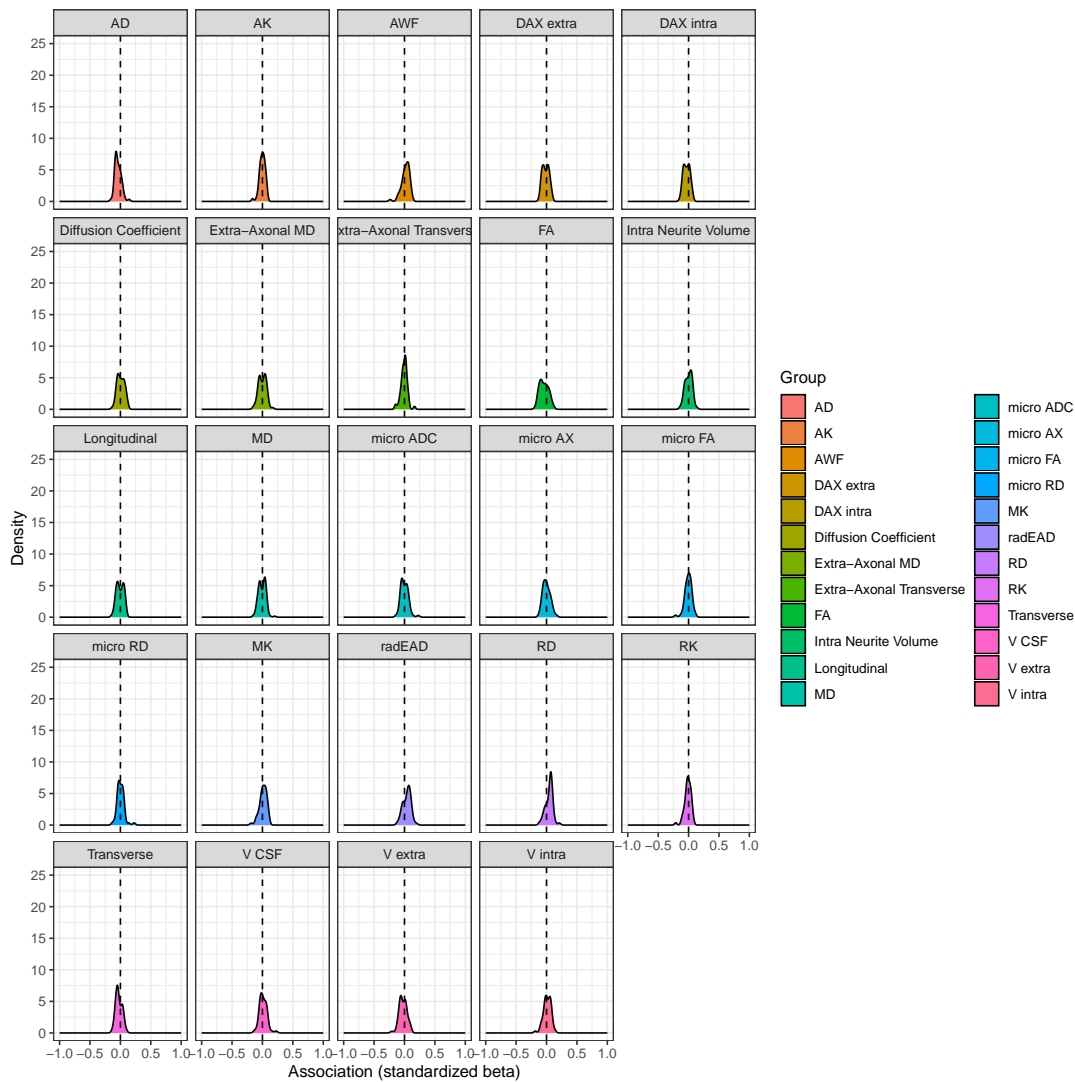
Supplementary Figure 9. T1w centercept BAG associations with the rate of change in T1w features
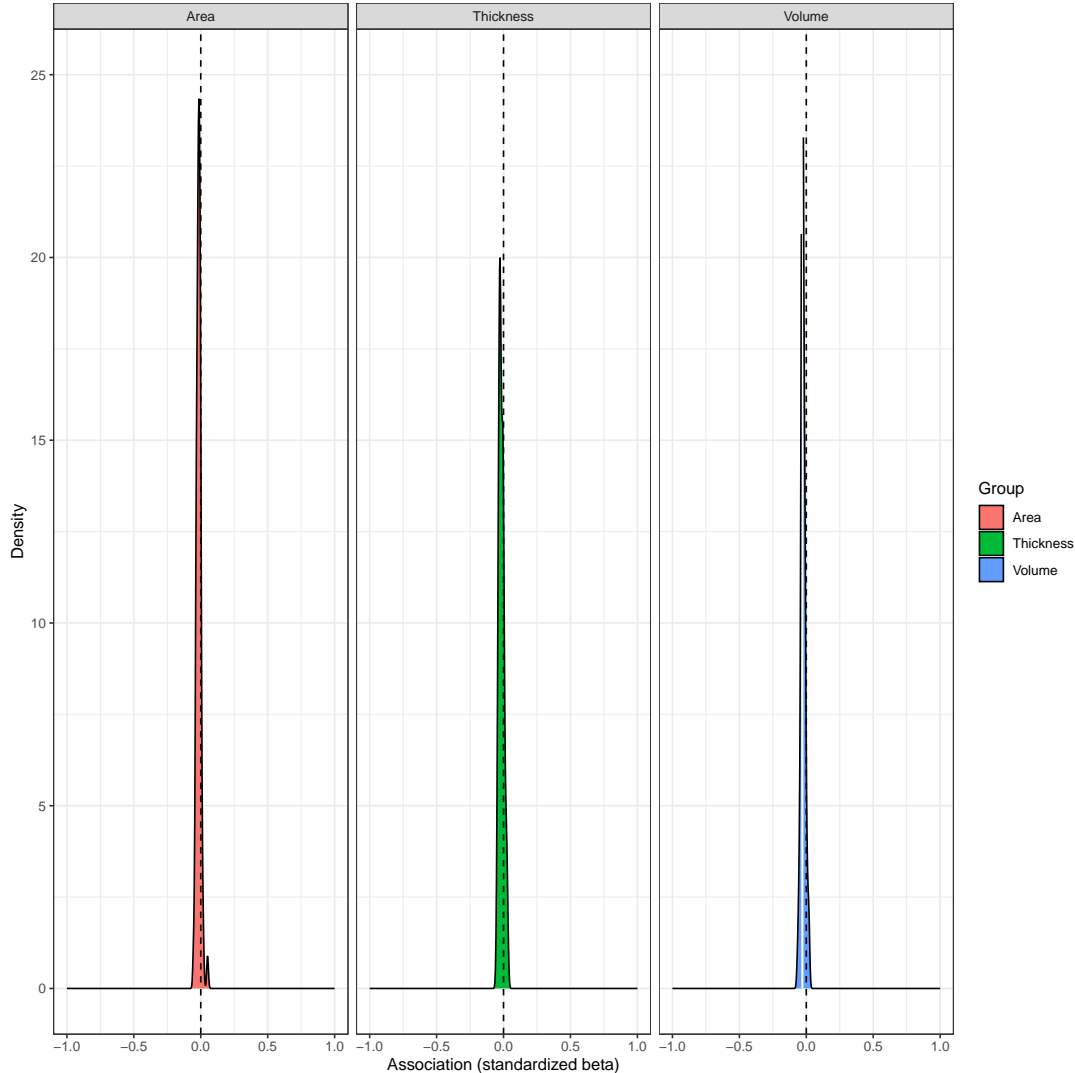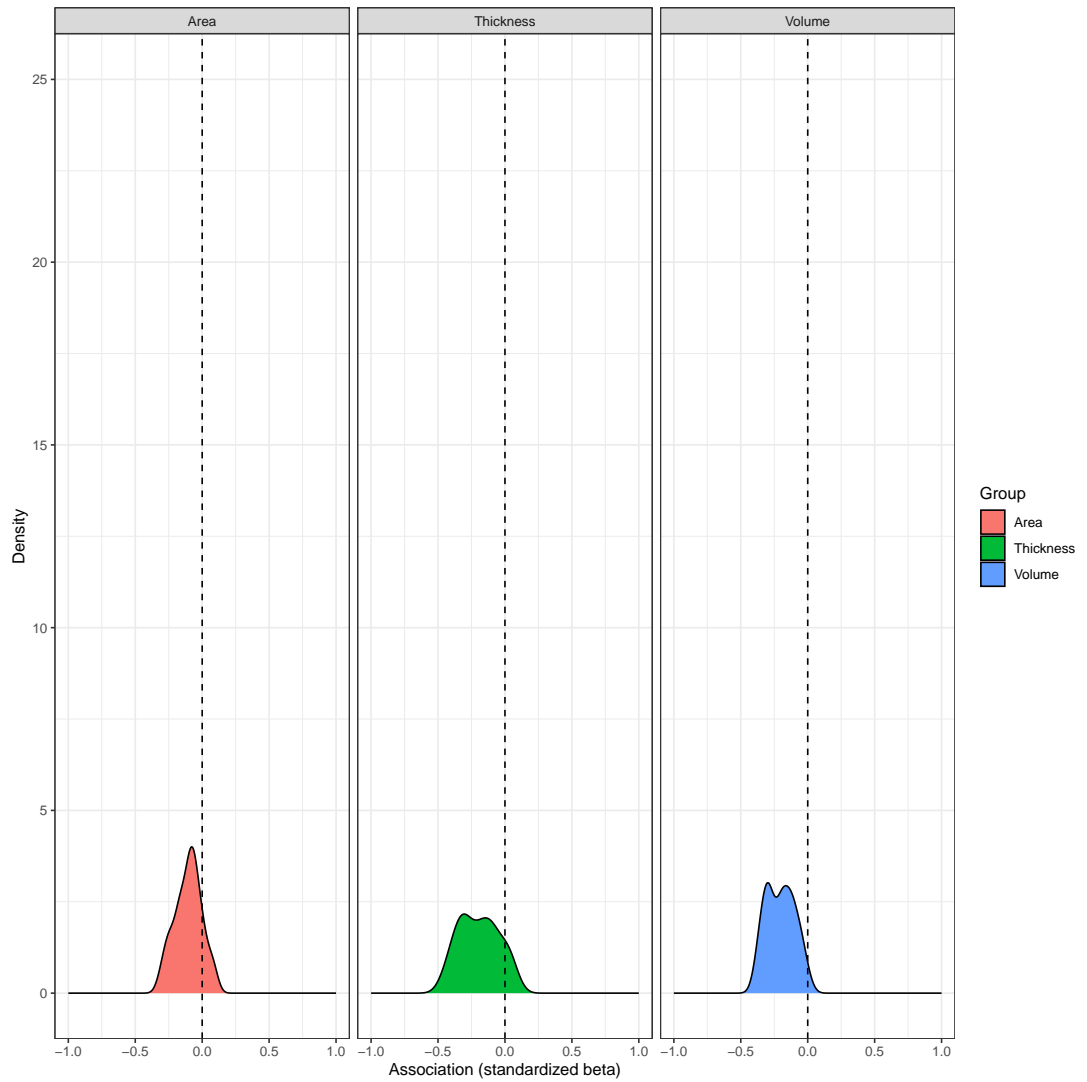
Supplementary Figure 10. Multimodal centercept BAG associations with the rate of change in multimodal features
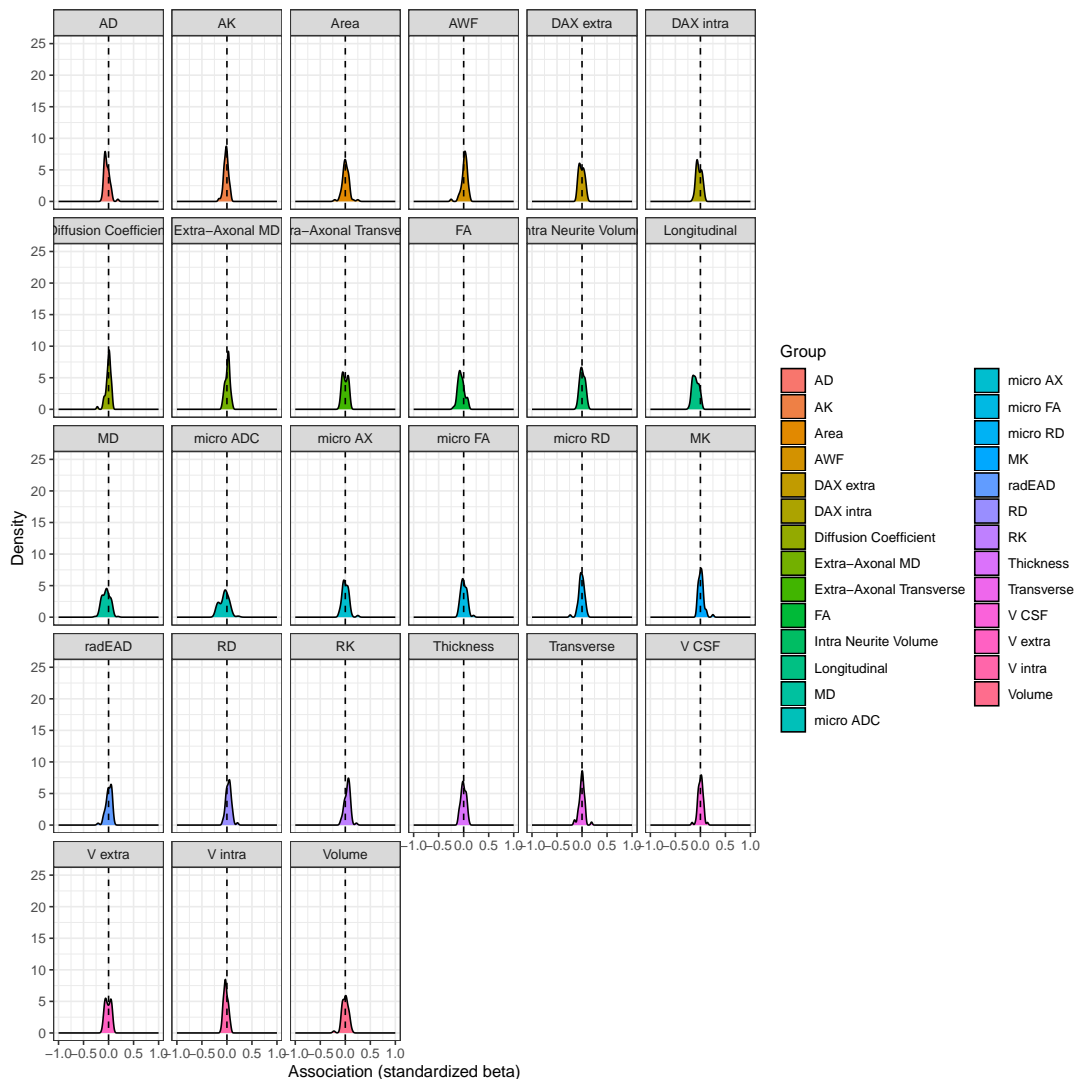
Supplementary Figure 11. dMRI annual rate of change in BAG associations with the rate of change in dMRI features
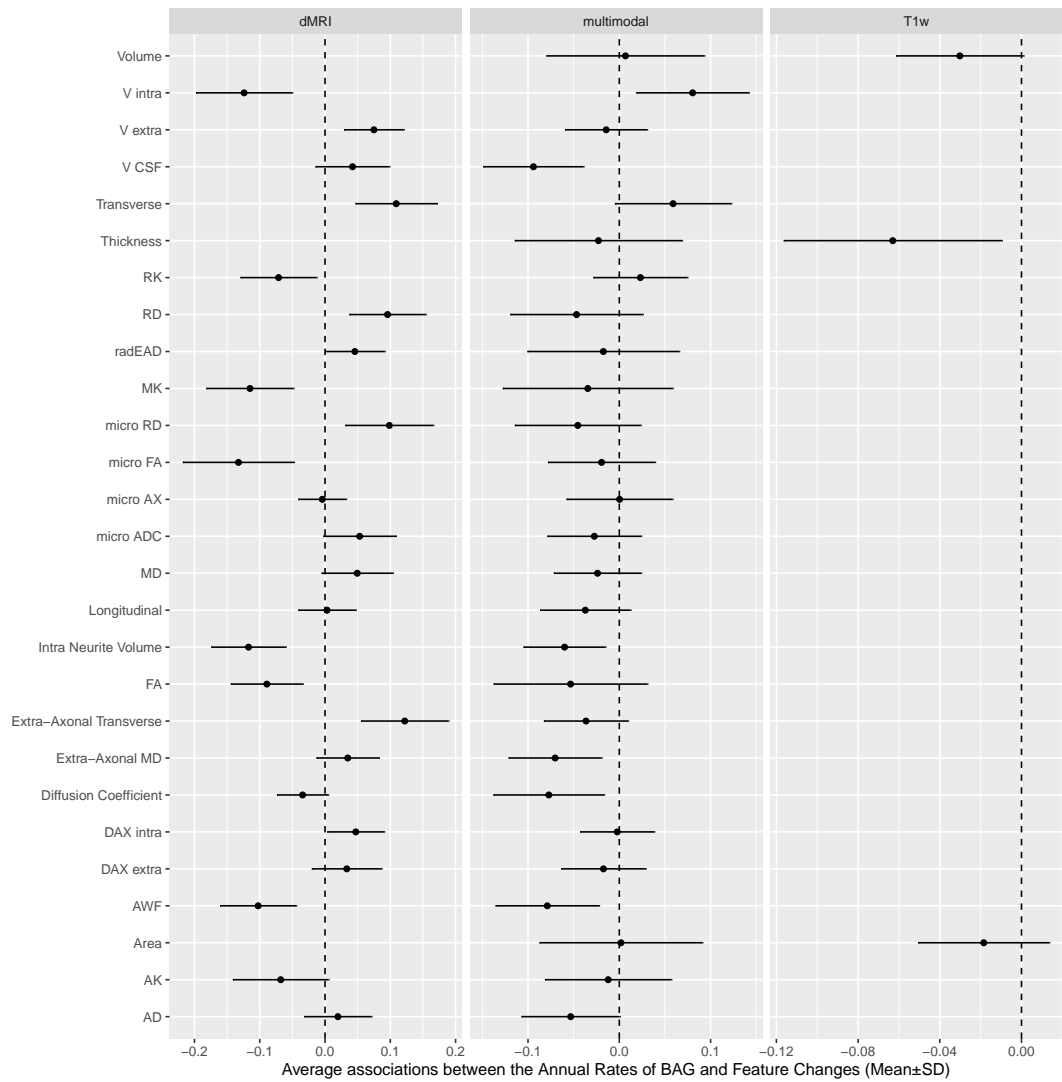
Supplementary Figure 12. T1w annual rate of change in BAG associations with the rate of change in T1w features

Supplementary Figure 13. Multimodal annual rate of change in BAG associations with the rate of change in multimodal features

Supplementary Figure 14. Average associations between the annual rate of change in BAG and the annual rate of change in multimodal features

Supplementary Figure 15. Average associations between the centercept of BAGs and the annual rate of change in multimodal features

Average associations between BAG Centercepts and the Annual Rate of Change per Feature (Mean±SD)
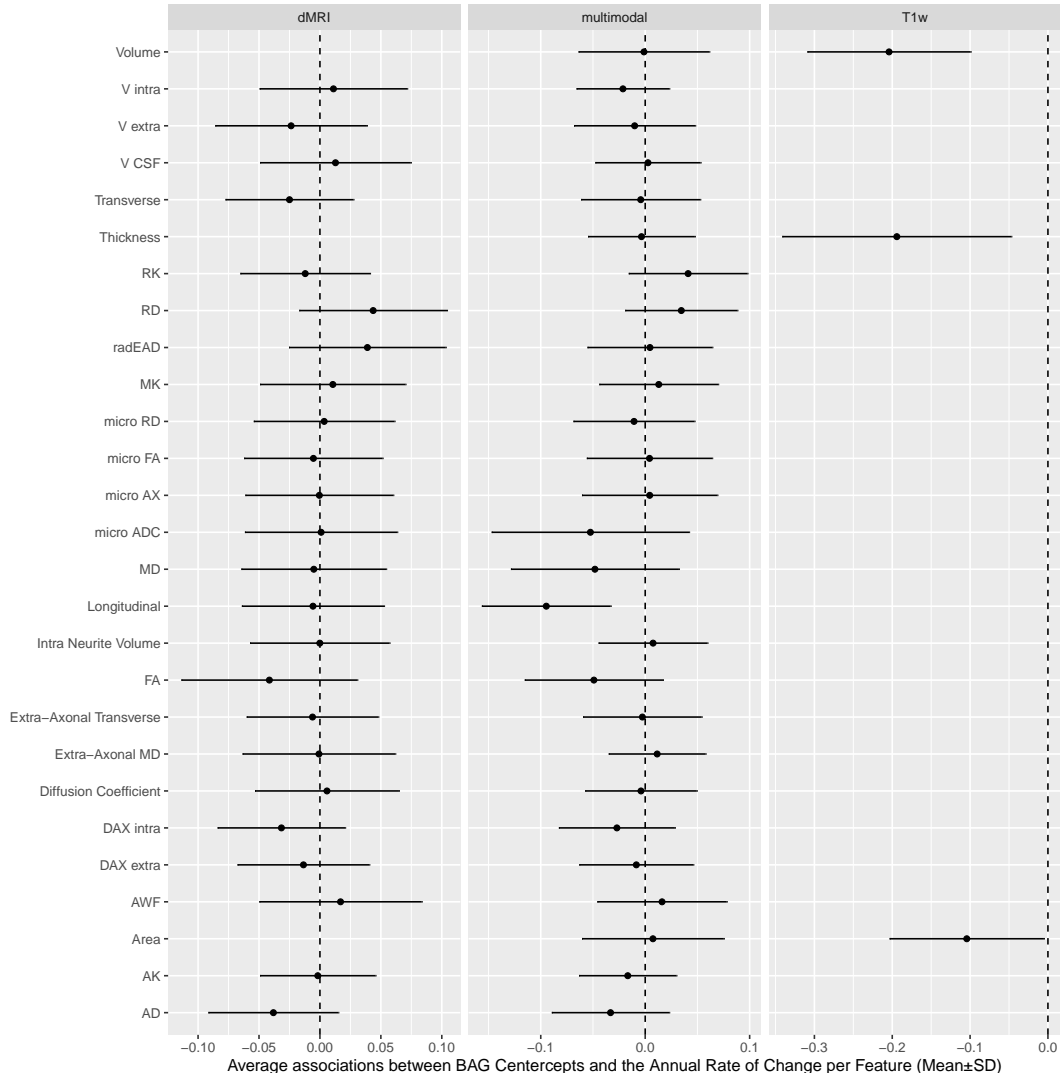
Supplementary Figure 16. Density of beta coefficients indicating associations between T_1-weighted centercept BAG and the rate of change in dMRI features

Supplementary Figure 17. Density of beta coefficients indicating associations between dMRI centercept BAG and the rate of change in T$_1$-weighted features

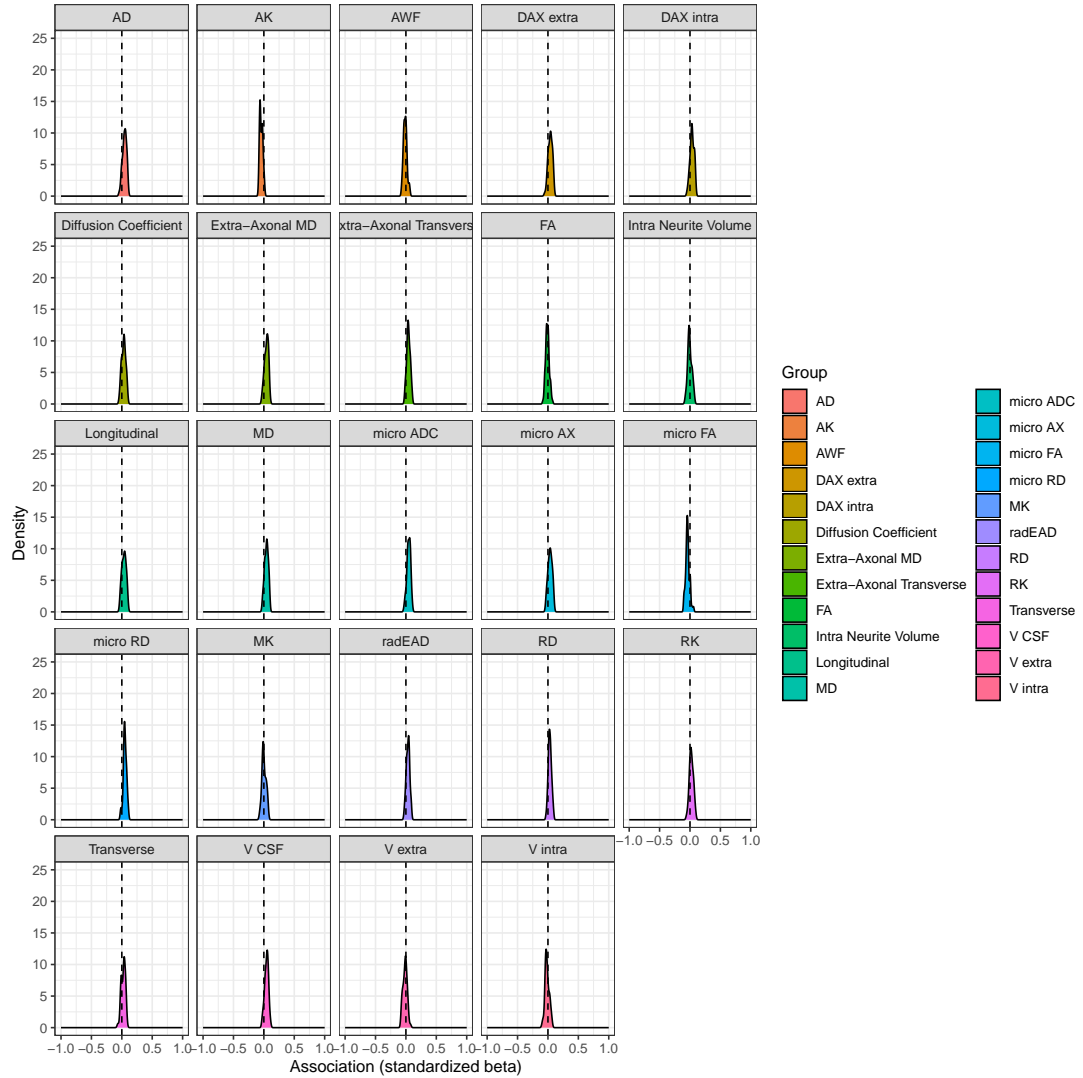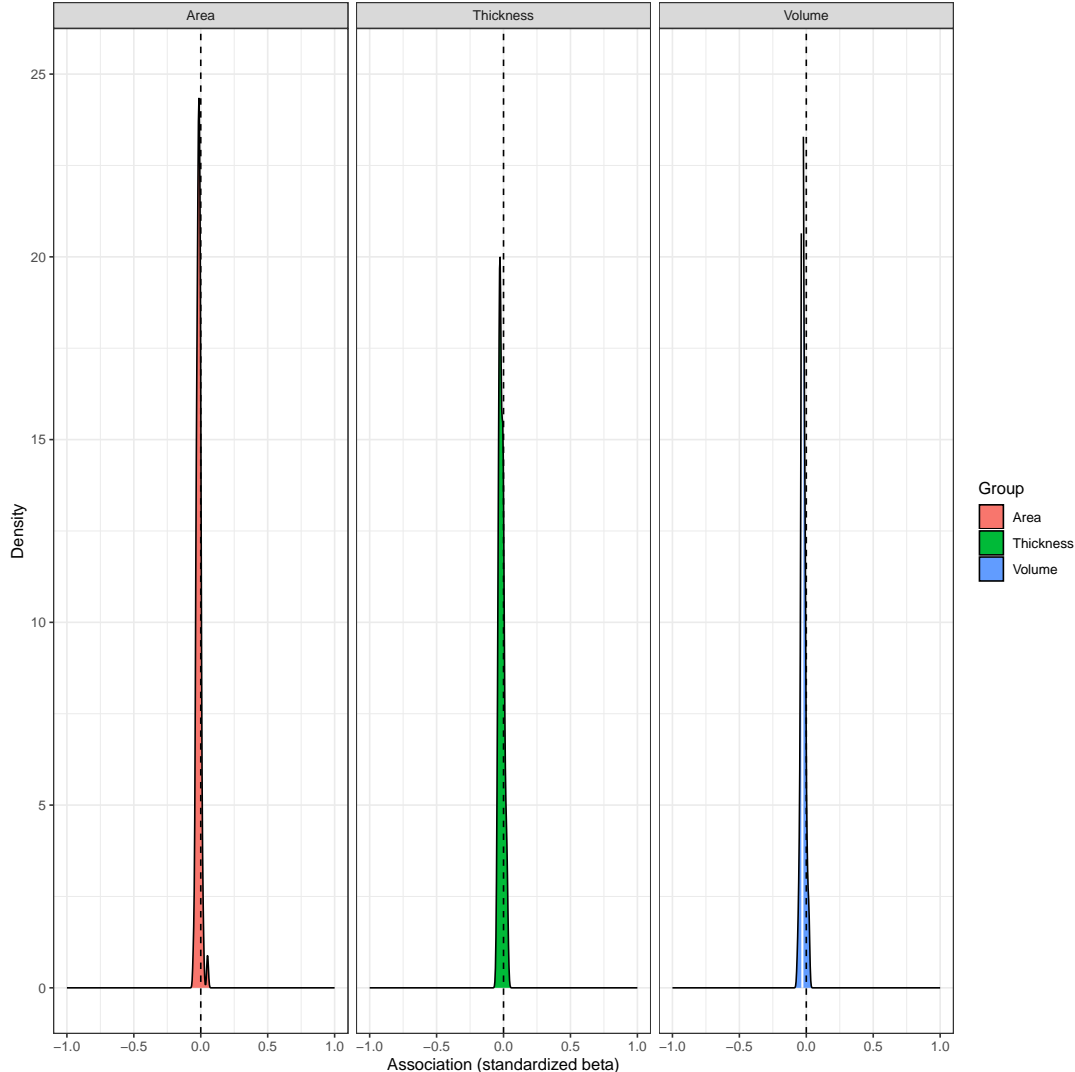**Supplementary Figure 18. Average associations between the annual rate of change in BAG and the annual rate of change in mu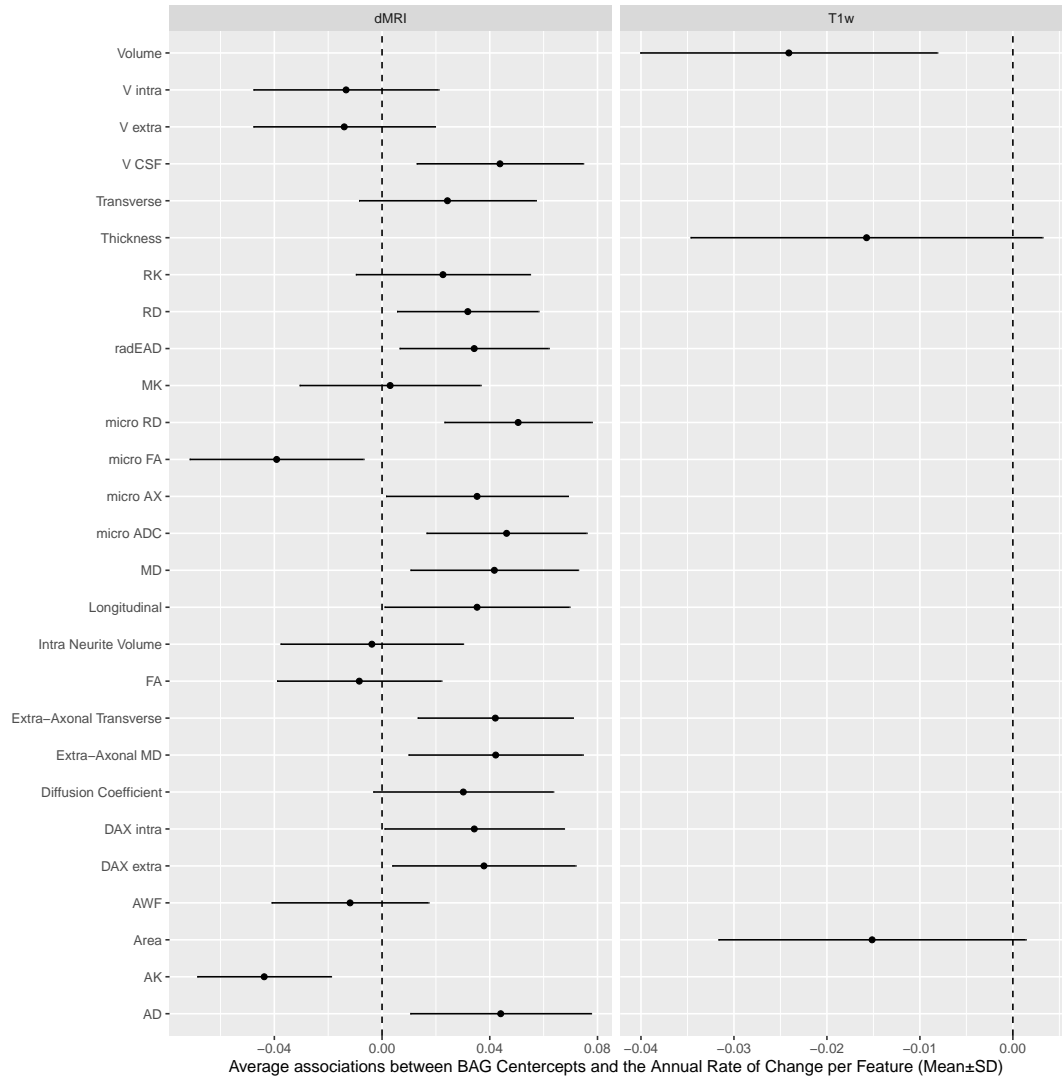ltimodal features predicting dMRI feature change from the T_1-weighted BAG centercept and T_1-weighted feature change from the dMRI centercept**

Average associations between BAG Centercepts and the Annual Rate of Change per Feature (Mean±SD)

Supplementary Figure 19. Time-point correlations of regional brain features.

Distribution of Brain Features' Correlations between Time 1 and 2

Mean Pearson's **r = 0.77**

Mean Pearson's **r = 0.86**

dMRI
T1w
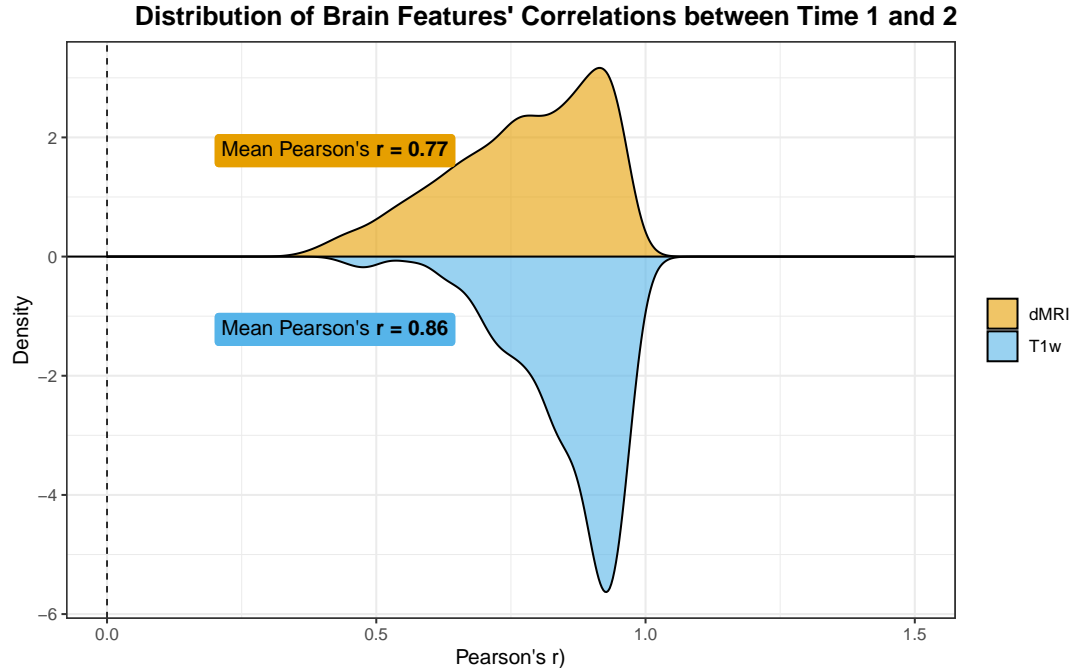
SUPPLEMENTARY NOTES

Supplementary Note 1. Independent prediction of brain age at each time point

After estimating the annual rate of change and centercepts for both brain age predictions and T_1-weighted features that changed significantly between time points, according to paired sample t-tests, we found similar percentages of variance explained across principal components of the centercept of features and the annual rate of change in features.
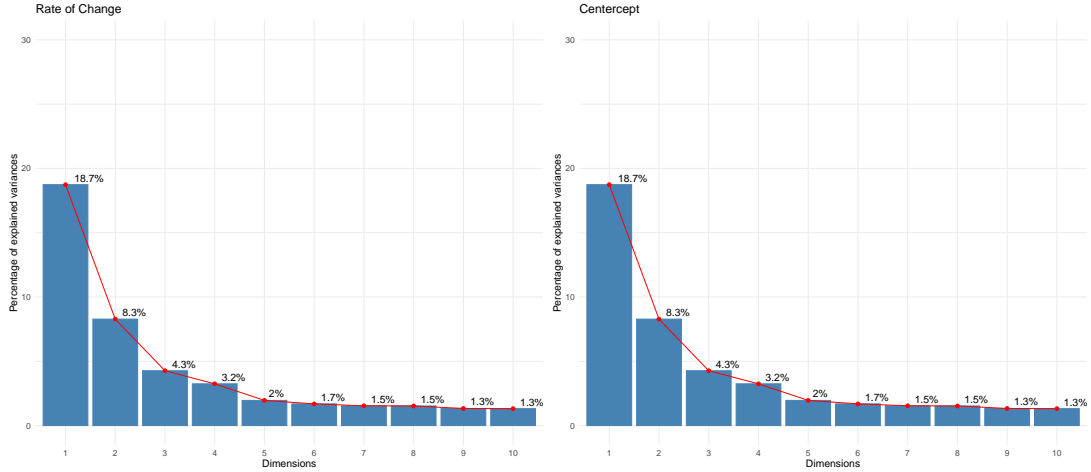
As in the main analyses, the cross-sectional proxies (BAG centercept) and longitudinal (annual rate of change) measures of BAG were strongly related to each other. Potentially due to the random split of training and testing data and the resulting difference of the inter-scan interval, features, etc. there was a strong correlation observable between the principal components of the rate of change and centercepts of brain features. These relationships appear similar when correcting for the inter-scan inter-

	Beta	Std. Beta	SE	t	p
corrected BAG	0.060	0.060	0.012	5.178	2.55×10^{-7}
uncorrected BAG	0.981	0.981	0.006	176.553	$<2.47\times10^{-324}$
PC	0.971	0.971	0.005	176.847	$<2.47\times10^{-324}$

val. As well as when testing these effects with non-linear interaction terms (cubic

	Beta	Std. Beta	SE	t	p
corrected BAG	0.057	0.057	0.009	6.348	2.55×10^{-10}
uncorrected BAG	0.980	0.980	0.003	341.399	$<2.47\times10^{-324}$
PC	0.964	0.964	0.003	308.530	$<2.47\times10^{-324}$

spline with k=4 knots). However, here the direction of the effect for the corrected BAG changed. Finally, we could also find a positive association between the centercept of

	Std.Beta	SE	t	p	F_smooth.Int	p.Interact
corrected BAG	-0.037	0.010	-3.700	0.0002	352.497	$<2.47\times10^{-324}$
uncorrected BAG	0.982	0.002	605.099	$<2.47\times10^{-324}$	1982.821	$<2.47\times10^{-324}$
PC	0.969	0.002	401.210	$<2.47\times10^{-324}$	960.369	$<2.47\times10^{-324}$

Table 2 Statistical Analysis Results

BAG and the rate of change principal components when using non-linear inter scan interval interactions with BAG, which is comparable to those reported in Suppl.Table 4.

	Std. Beta	SE	t	p	F_{smooth}	Int	$p_{Interact}$
CCu_AROC_	0.266	0.033	8.124	9.31×10^{-16}	6.652	0.007	
CCc_AROC_	0.200	0.026	7.640	3.83×10^{-14}	4.388	0.019	

Supplementary Note 2. Analysis protocol

1. Data processing and extraction of region-wise metrics/features, QC. Resulting data: a large cross-sectional training data set and a longitudinal data set with two time point serving as test data. We differentiate data in diffusion MRI derived metrics only, T1-weighted MRI derived metrics only, and their combination, labelled as multimodal MRI data.
2. Training of brain age models from these features, using XG Boost, Lasso, and linear models.
3. Assessment of the trained models based on predictions in training and test samples. Selection of the best-performing models.
4. Predictions in test data were obtained. Additionally, the predictions were corrected by the slope of linear models associating age and brain age. This results in uncorrected and corrected brain age estimates.
5. Brain age gaps (BAG) were estimated from these estimates by subtracting chronological age from the brain age estimates.
6. For the analyses, we first estimate the time point differences and correlations between time point specific BAGs.
7. We then assessed the effects of feature changes using t-tests and quantify the effects using Cohen's d. We average the obtained d values by modality (dMRI, T1-weighted, multimodal MRI) and then by metric (e.g., volume, surface area, fractional anisotropy).
8. For the significantly changing features the centercept and the annual rate of change in the features were estimated.
9. The resulting centercept and rate of change feature-level metrics were used to estimate principal components of which we used the first component each: one

component reflecting the centercept, one reflecting the annual rate of change in features.

10. Similarly, we estimated the centercept (as predictor) and annual rate of change of BAGs which were associated with each other.

11. Additionally, the centercept (as predictor) and annual rate of change of PCs were associated with each other.

12. As a control, the same two analyses above were executed using the inter scan interval to be interacted with the centercept.

13. Then, we associated the centercepts of BAG with the annual rate of change in the PCs, both within modality (e.g., BAG_{dMRI} and ΔBAG_{dMRI})) and between modalities (e.g., BAG_{dMRI} and ΔBAG_{T1w})).

14. As a final step, we associated the centercepts and annual rates of changes in BAGs and PCs with the centercepts and annual rates of changes of the features which significantly changed over time.

REFERENCES

[1] Reisert, M., Kellner, E., Dhital, B., Hennig, J. & Kiselev, V. G. Disentangling micro from mesostructure by diffusion MRI: a Bayesian approach. *Neuroimage* **147**, 964–975 (2017).

[2] Jensen, J. H., Helpern, J. A., Ramani, A., Lu, H. & Kaczynski, K. Diffusional kurtosis imaging: the quantification of non-gaussian water diffusion by means of magnetic resonance imaging. *Magnetic Resonance in Medicine: An Official Journal of the International Society for Magnetic Resonance in Medicine* **53**, 1432–1440 (2005).

[3] Fieremans, E., Jensen, J. H. & Helpern, J. A. White matter characterization with diffusional kurtosis imaging. *Neuroimage* **58**, 177–188 (2011).

[4] Basser, P. J., Mattiello, J. & LeBihan, D. Mr diffusion tensor spectroscopy and imaging. *Biophysical journal* **66**, 259–267 (1994).

[5] Kaden, E., Kruggel, F. & Alexander, D. C. Quantitative mapping of the per-axon diffusion coefficients in brain white matter. *Magnetic resonance in medicine* **75**, 1752–1763 (2016).

[6] Kaden, E., Kelm, N. D., Carson, R. P., Does, M. D. & Alexander, D. C. Multi-compartment microscopic diffusion imaging. *NeuroImage* **139**, 346–359 (2016).

[7] Maximov, I. I. *et al.* Fast qualitY conTrol meThod foR derIved diffUsion Metrics (YTTRIUM) in big data analysis: UK Biobank 18,608 example. *HBM* **42**, 3141–3155 (2021).